

Watershed Erosion Modeling with CASC2D-SED

Pierre Julien

Professor of Civil Engineering, Engineering Research Center, Colorado State University, Fort Collins, CO 80523, pierre@engr.colostate.edu

Rosalía Rojas

Ph.D. candidate, Civil Engineering Dept., Colorado State University, Fort Collins, CO 80523

Abstract. Developed at Colorado State University, CASC2D-SED is a physically-based model simulating the hydrologic response of a watershed to a distributed rainfall field. The time-dependent processes include: precipitation, interception, infiltration, surface runoff and channel routing, upland erosion, transport and sedimentation. CASC2D-SED is applied to Goodwin Creek, Mississippi. The watershed covers 21km² and has been extensively monitored both at the outlet and at several internal locations by the ARS-NSL at Oxford, MS. The model has been calibrated and validated using rainfall data from 16 meteorological stations, 6 stream gaging stations and 6 sediment gaging stations. Sediment erosion/deposition rates by size fraction are predicted both in space and time. Geovisualization, a powerful data exploration technique based on GIS technology, is used to analyze and display the dynamic output time series generated by the CASC2D-SED model.

1. Introduction

Erosion and sedimentation embody the processes of detachment, transport, and deposition of soil particles. Erosion and subsequent deposition can cause major problems. Erosion reduces productivity of cropland, sediment degrades water quality and may carry soil adsorbed polluting chemicals. Deposition in irrigation canals, stream channels and reservoirs reduces structural capacity and requires costly removal.

Ideally, an erosion model should describe the physical processes controlling erosion, and the model parameters should be directly related to measurable physical properties (Lane et al., 1988). Soil erosion computer models can be theoretical, physically based, or empirical. Most erosion models are of a hybrid type including both theoretical and empirical components (Haan et al., 1994).

In recent years, Geographical Information System (GIS) applications in environmental modeling have proliferated to take advantage of the spatial data representation capabilities. In hydrology, 2-D physical models are replacing simple 1-D representation of surface flow processes in catchment models. In erosion models, 2-D studies enable the identification of vulnerable regions within a watershed, thus facilitate improvement in the planning of soil conservation systems.

Developed at Colorado State University, CASC2D-SED is a physically-based raster hydrologic model which simulates the hydrologic response of a watershed subject to a distributed rainfall field (Julien et al., 1995; and Johnson et al., 2000). Major hydrologic processes vary in time and space to describe: precipitation, interception, infiltration, Hortonian runoff, runoff and channel routing and upland erosion and sedimentation.

The objective of this paper is to show applications of the model CASC2D-SED to Goodwin Creek, Mississippi. The 21 km² watershed is extensively monitored by the ARS-NSL at Oxford, MS.

2. Soil erosion and GIS

Soil erosion is influenced by the spatial heterogeneity in topography, vegetation, soil type, and land use. This is where a Geographical Information System (GIS) becomes a valuable tool. Particularly, the importance of using Digital Elevation Models (DEM) to represent the topography of watersheds is recognized. Erosion potential prediction is becoming a more and more widely applied GIS operation (Mitchell et al., 1993; De Roo, 1996; Mitasova et al., 1996, Molnar and Julien, 1998). The redistribution of sediment will drive the long-term landscape change, which in turn will affect the hydrological processes acting within and over individual hillslopes (Brooks and McDonnell, 2000).

Visualization of geographical information (geovisualization) is a powerful data exploration technique, exploiting the ability of current computing technology to analyze and display dynamically large amounts of information (Edsall et al., 2000). Geovisualization involves the use of computer graphics to stimulate the human visual system to recognize patterns that would not otherwise be obvious. Visualization techniques are applied to scientific research in two ways: (1) as visual thinking or cognitive visualization, for exploration and verification of spatial data, and (2) as visual communication, where the scientist communicates with other people to present and discuss results (Dransch, 2000).

Time-series animation is a visualization technique ideally suited for displaying temporal geographic data. Animation leads to faster and easier comprehension of spatial patterns, trends and rates of change of data (Acevedo and Masuoka, 1997).

3. CASC2D-SED description

3.1. Model formulation

For a given rainfall event, once the interception has been subtracted from rainfall, water begins to infiltrate. The Green & Ampt (1911) infiltration equation is used to accommodate spatial and temporal variabilities due to changes in the rainfall and/or soils properties, and taking into account the accumulated infiltration. When the precipitation rate exceeds the infiltration rate, the excess rainfall will accumulate as surface water and begin to flow at a depth greater than the retention depth. Overland flow is routed into the channels using a diffusive wave approximation in two dimensions. In channels, the water is routed using a 1-D diffusive wave equation. The erosion and sedimentation rates are calculated as a function of the hydraulic properties of the flow, the physical properties of the soil and the surface characteristics. The modified Kilinc-Richardson equation (Julien, 1995) is used in CASC2D-SED to determine the upland sediment transport by grain size (sand, silt, and clay) from one cell into the next one in two orthogonal

directions. The sediment coming from upland erosion is routed through channels and into the outlet using the Engelund and Hansen (1967) transport equation.

In CASC2D-SED, geospatial data are input as raster maps (grids). Watershed relief is represented with a DEM. Slope values and channel network are derived from this DEM. Channel characteristics are taken from surveys or from remote sources. The soil and land use /land cover (LULC) grids are reclassified to infer CASC2D parameter values related to interception, infiltration, roughness coefficients, and erosion. Input rainfall grids are calculated by interpolating rainfall rates in spatially distributed raingages.

CASC2D-SED output include: (1) a summary file containing information on the simulation parameters, channel topology inferred from the link and node maps and the final results of the hydrological and erosion components; (2) flow and sediment flow files: containing the water flow and sediment flow at the outlet. Results can optionally be written at other internal locations inside the watershed; and (3) time-series grids: these are optional and represent simulation values at predetermined times (regular intervals). Output raster maps include the distribution of: rainfall rate, accumulated infiltration depth, surface flow depth, total sediment volume, suspended sediment volume, and sediment flux and concentration by size fraction, and net erosion and sedimentation.

3.2. Governing equations

The governing equations corresponding to the processes of precipitation, interception, infiltration, overland and channel flow routing are described in Julien and Saghafian (1991). The governing equations corresponding to the erosion and deposition processes follow.

3.2.1. Upland erosion. The equation of Kilinc and Richardson (1973) used in CASC2D-SED to estimate sheet and rill erosion in bare soils:

$$q_s = e^{11.727} S_o^{1.664} q^{2.035} \quad (1)$$

where

$$\begin{aligned} q_s &= \text{unit sediment discharge [lb/ft s]} \\ S_o &= \text{terrain slope [ft/ft]} \\ q &= \text{unit flow discharge (ft}^2\text{/s)} \end{aligned}$$

In the more general case of erosion from sheet flow, modifications to the last equation reflect the influence of soil type, vegetation, and practice factor using the USLE factors K_{USLE} , C_{USLE} , and P_{USLE} as (Julien, 1995):

$$q_{KR} = 23210 S_o^{1.66} q^{2.035} \frac{K_{USLE}}{0.15} C_{USLE} P_{USLE} \quad (2)$$

where :

$$\begin{aligned} q_{KR} &= \text{unit sediment discharge [tons/m s]} \\ q &= \text{unit flow discharge [m}^2\text{/s]} \\ K_{USLE} &= \text{dimensionless erodibility factor in the USLE equation} \\ C_{USLE} &= \text{cropping management factor in the USLE equation} \\ P_{USLE} &= \text{conservation practice factor in the USLE equation} \end{aligned}$$

After computing the unit sediment discharge, the upland erosion is calculated for three size fractions: sand, silt and clay (Johnson et al., 2000). These fractions are routed based upon the amount of sediment in suspension and from previous deposition (see Figure 1). The suspended sediment is transported by size fraction proportionally to the amount of this size fraction in the suspended sediment. If the transport capacity is greater than the volume of suspended sediment, the previously deposited sediment is transported by size fraction, again, proportionally to the amount of the given size fraction in the deposited sediment. Subsequent excess transport capacity corresponds to erosion of the parent soil with size fractions in proportion to the soil texture.

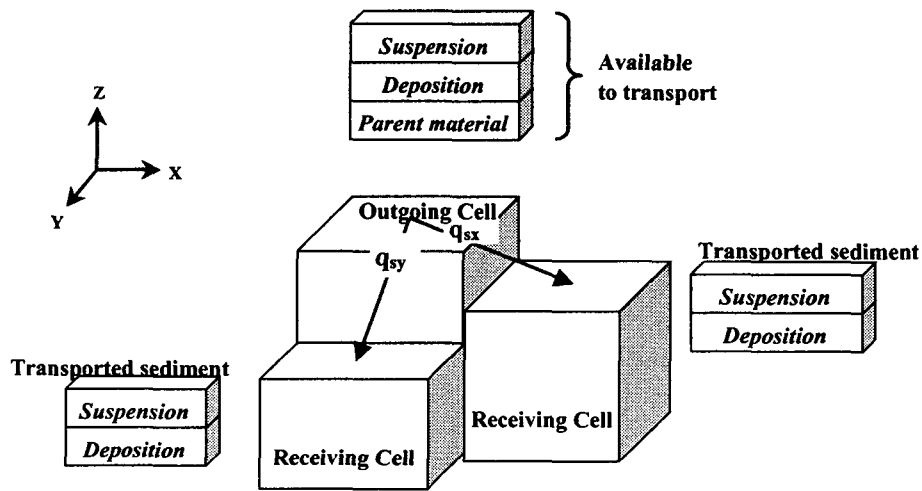


Figure 1. Schematic of upland erosion scheme (Johnson et al., 2000)

3.2.2. Channel sediment transport. The eroded material in the upland portion of the watershed is transported to the outlet through the channels. Currently, in CASC2D-SED, erosion is not allowed to occur in the channels. Thus, transport might be supply limited. Deposition of material is allowed. Like for the routing of the sediment in the overland portion, the transport capacity if fulfilled, first, with the suspended sediment volume and, if needed, with the previously deposited sediment.

The Engelund and Hansen (1967) equation is used to calculate the sediment transport capacity in the channels by size fraction, i . Engelund and Hansen applied Bagnold's stream power concept and the similarity principle to obtain the sediment concentration by weight for size fraction i (C_{wi}) as follows (Julien, 1995):

$$C_{wi} = 0.05 * \left(\frac{G}{G-1} \right) * \frac{V * S_f}{\sqrt{(G-1) * g * d_{si}}} * \sqrt{\frac{Rh * S_f}{(G-1) * d_{si}}} \quad (3)$$

where:

- G = specific gravity of sediment [--]
- V = channel depth-averaged velocity [m/s]

- Sf = channel friction slope [m/m]
 g = gravitational acceleration [m/s²]
 dsi = size fraction i [m]
 Rh = channel hydraulic radius [m]

and the sediment transport capacity corresponding to size fraction i is calculated with the Engelund and Hansen equation as:

$$Q_{EH_i} (m^3/s) = Q * Cwi / 2.65 \quad (4)$$

where Q is the flow discharge [m³/s] in the channel.

Once the sediment is brought into suspension, the suspended size fraction moves by advection. The advective fluxes describe the transport of sediment imparted by velocity currents. This implies that sediment will move with the fluid even when the transport rate is lower or higher than the transport capacity. Thus, we have a supply limited transport condition in some cases, and a capacity limited transport condition in others. The rate of mass transport carried by advection, Q_{ADV_i} [m³/s] is obtained from the product of sediment concentration and the velocity component (Julien, 1995):

$$Q_{ADV_i} = A * V * Ci \quad (5)$$

where:

- Q_{ADV_i} = size fraction i sediment transport [m³/s]
 A = flow area [m²]
 V = depth-averaged flow velocity [m/s]
 Ci = suspended size fraction i concentration [m³/m³]

The excess transport capacity is defined as the flow capacity to move the bed-material once the sediment transported by advection is subtracted. For each size fraction, the amount of bed-material that will be transported is limited by the amount that can be transported by the flow (advection) or by the excess transport capacity. The excess capacity, expressed as a volume, to carry size fraction i channel bed-material, $XSScap_i$, is found as:

$$XSScap_i = MAX \left\{ 0, (Q_{EH_i} - Q_{ADV_i}) * dt \right\} \quad (6)$$

while the volume of fraction i bed-material that can be transported by advection in the channel is:

$$BMvol_i * \frac{V * dt}{W} \quad (7)$$

where $BMvol_i$ is the volume of size fraction i found in the bed-material. The volume of size i bed-material that will be transported from the bed-material, $qsBM_i$, is found to be the minimum between the excess capacity and the volume of the bed-material that can be carried by advection for that size fraction:

$$qsBM_i = MIN \left\{ XSScap_i, BMvol_i * \frac{V * dt}{W} \right\} \quad (8)$$

In the case in which there is still remaining transport capacity, this will not be used, as channels are not currently allowed to erode in CASC2D-SED.

3.2.3. Sediment settling. Once sediment has been routed in overland and channel cells, the suspended sediment portion is allowed to deposit. The

percentage of suspended sediment fraction, $PercSett_i$, that is allowed to settle depends on the fall velocity corresponding to the median size fraction diameter, w_i , elapsed time (i.e. computational time step, dt) and water depth (d) in the cell.

$$\begin{aligned} PercSett_i &= w_i * dt * d^{-1} && \text{if } d > w_i * dt \\ PercSett_i &= 1 && \text{otherwise} \end{aligned} \quad (9)$$

Deposit is thus allowed to deposit for no flow conditions, like for example in DEM sinks.

4. Field application

4.1. Site description

The model CASC2D-SED is applied to the Goodwin Creek watershed in Mississippi for comparison with field measurements of surface runoff and sediment discharge at the outlet and at other internal locations within the basin.

Goodwin Creek, MS, (see Figure 2) is operated by the ARS-National Sedimentation Laboratory (NSL), and is organized and instrumented for conducting extensive research on upstream erosion, instream sediment transport, and watershed hydrology (Alonso, 1996; Kuhnle and Willis, 1998). The watershed has a database compiling runoff, sediment, and precipitation from 1981 until 1996. Channel cross-section data is compiled from 1978 until 1988¹.

The watershed flows approximately from northeast to southwest, draining a total area of 21.4 km². The terrain elevation ranges from 71 m to 128 m above mean sea level, with an average channel slope of 0.004 in Goodwin Creek. The Digital Elevation Model (DEM) of Goodwin Creek is found in Figure 3.

The climate of the watershed is humid, hot in summer and mild in winter. The average annual rainfall during 1982-1992 from all storms was 1440 mm, and the mean annual runoff measured at the watershed outlet was 145 mm per year.

In Goodwin Creek, two major soil associations are mapped. The Collins-Fallaya-Grenada-Calloway association is mapped in the terrace and flood plain locations. These are silty soils, poorly to moderately well-drained, and cover most of the cultivated area in the watershed. The Loring-Grenada-Memphis association has developed on the loess ridges and hillsides. These are well to moderately well-drained soils on gently sloping to very steep surfaces and include most of the pasture and wooded area in the watershed (Blackmarr, 1995). The Goodwin Creek soils map is found in Figure 3.

The land use and management practices influence the rate and amount of sediment delivered to streams from the upland. They range from timbered areas to row crops. The Goodwin Creek watershed is largely free of land management activities with 13 percent of its total area being under cultivation and the rest in idle, pasture and forestland. The land use map is presented in Figure 3. LULC in Goodwin Creek are classified as cultivated land, pasture,

¹ This database is available at http://www.sedlab.olemiss.edu/cwp_unit/Goodwin.html

idle land, forest, and planted forest (Blackmarr, 1995). In this study, the LULC has been further reclassified as forest (includes planted forest), pasture (includes idle land), water and cultivated.

The digital elevation map, soil type map and LULC map are available at 30-m resolution. Figure 3 shows these maps. They will be used as input in the CASC2D-SED program.

The Goodwin Creek Watershed is divided into fourteen nested sub-catchments with a flow-measuring flume constructed at each of the drainage outlets. The drainage areas above these stream-gaging sites range from 1.63 to 21.3 km². Twenty-nine standard recording raingages are uniformly located within and just outside the watershed (Blackmarr, 1995). Figure 2 shows the watershed location, channel network and raingages location.

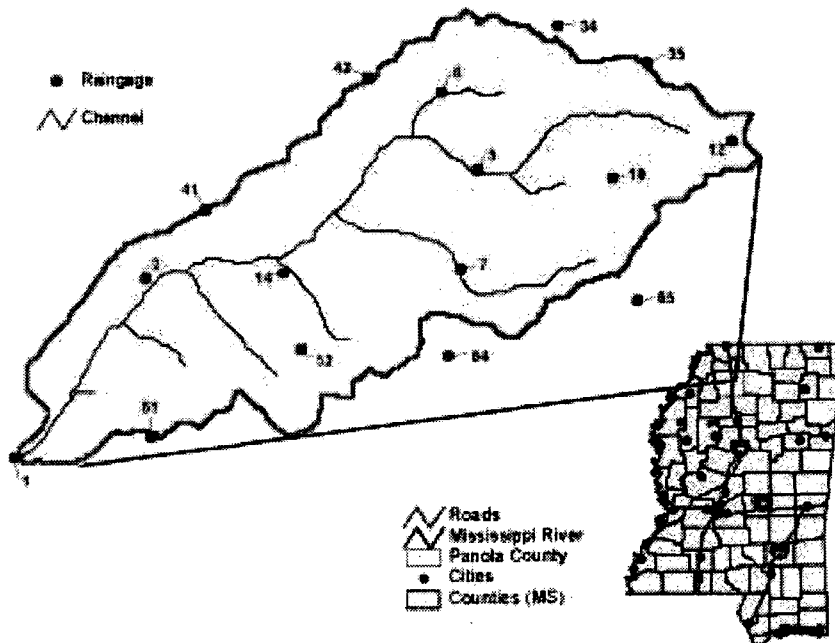


Figure 2. Goodwin creek location, raingage locations and channel network.

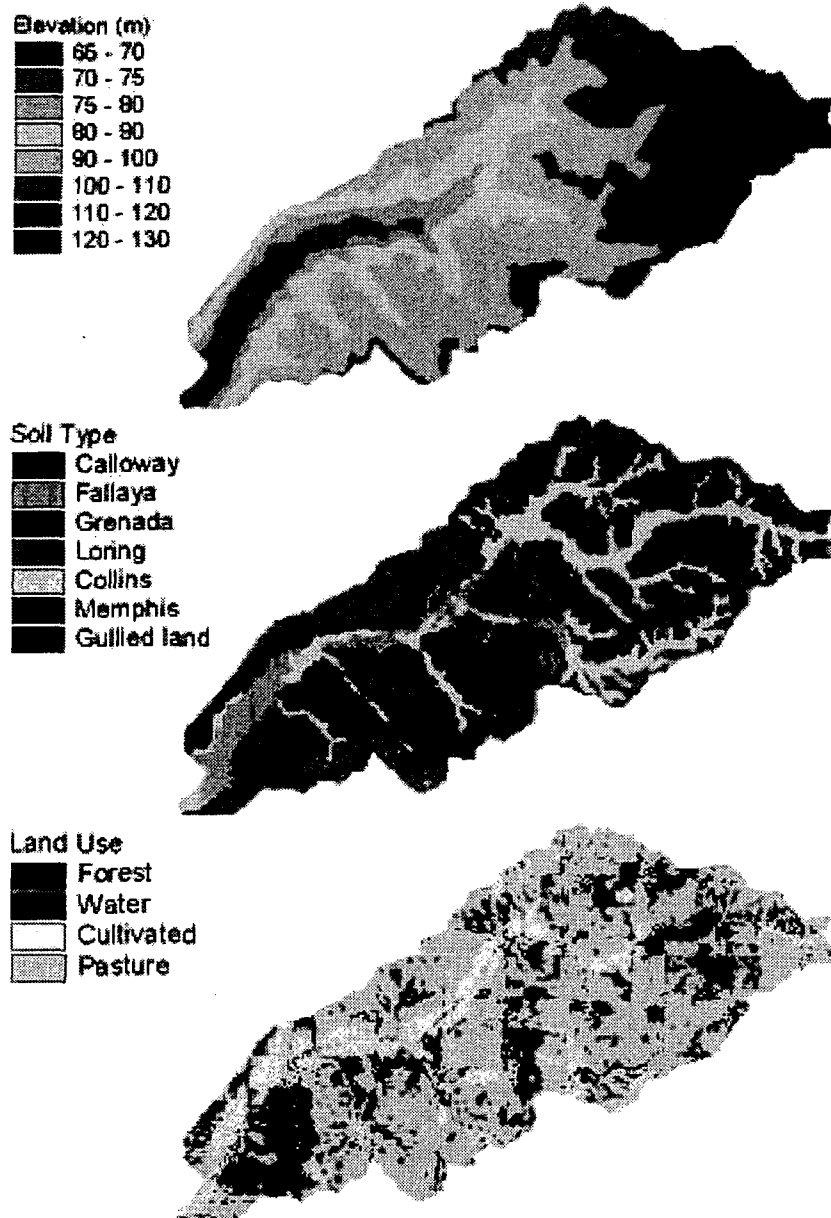


Figure 3. Goodwin Creek elevation, soil type and land use maps.

4.2. Input data

4.2.1. Precipitation. The storm event of October 17, 1981 began at 9:19 p.m. with a total rainfall duration of 3.5 hours and with very little rainfall preceding this event. Precipitation data from 16 raingages have been used within and just outside the watershed (see Figure 2). The total rainfall for this event varied from 5.7 to 7.9 cm with an average value of 7.2 cm.

4.2.2. Infiltration parameters. The infiltration parameters are derived from the soil type map. Average infiltration parameters of saturated hydraulic

conductivity (K_s) and suction head (G) have been taken from Rawls et al. (1983). Soil moisture deficit (Md) has been estimated from soil porosity, residual moisture and antecedent rainfall events. The calibrated infiltration parameter values are shown in Table 1.

4.2.3. Channel parameters. The channel network is derived from the resampled, smoothed DEM for a minimum flow accumulation of 40.5 has. The resulting network is very similar to that provided by the ARS and is shown in Figure 2. The channel topology thus defined is input into CASC2D-SED in the form of two raster maps: a link map in which the channel link number is defined for each grid cell, and a node map where each link nodes are numbered. Channel characteristics have been taken from Blackmarr (1995). A constant value of the roughness coefficient, $n = 0.035$, has been estimated for all the channel links

4.2.4. Roughness parameters. The roughness coefficient is derived from the LULC map and its value is taken from Woolhiser (1975). See Table 1 for calibration run values.

4.2.5. Erosion parameters. Percentages of particle fraction and the USLE erodibility factor (K_{USLE}) are derived from the soil type map. The USLE cover factor (C_{USLE}) and management practice factor (P_{USLE}) are derived from the land LULC map. The average percentages of sand and silt and particle size for a silty-loam soil are taken from the USDA (1975) texture triangle. The K_{USLE} , C_{USLE} and P_{USLE} values are taken from Wischmeier and Smith (1978). See Table 1 and

Table 2 for calibration run values.

Table 1. Soil infiltration and erosion parameter values for the test run

Soil Series	Drainage condition	K_s [cm/s]	G [cm]	Md [cm ³ /cm ³]	K_{USLE}	% Sand	% Silt
Calloway	Poor	0.450	28	0.35	0.4	25	55
Fallaya	Poor	0.450	28	0.37	1	30	60
Grenada	Moderate	0.350	20	0.35	0.4	25	55
Loring	Mod/well	0.350	28	0.32	0.4	25	55
Collins	Mod/well	0.220	20	0.35	0.3	30	60
Memphis	Well	0.500	25	0.33	0.1	25	55
Gullied Land	Poor	0.220	15	0.38	0.1	25	55

Table 2. Land use parameter values for the test run.

Land Cover	Roughness	Interception [mm]	C_{USLE}	P_{USLE}
Forest	0.25	3	0.001	1
Water	0.01	0	0	1
Cultivated	0.15	1	0.1	1
Pasture	0.2	1.5	0.02	1

5. Results

The runoff event on October 17, 1981 was calibrated for the 30-m resolution grid. Outflow results for the described event show that CASC2D-SED is able to simulate the overall shape of the hydrograph, peak flow and time to peak at the basin outlet (see Figure 4). At internal locations this is also true but for the smaller sub-basins, where the peak flows are sometimes under-predicted due to spatial rainfall patterns and the rapid translation of rainfall rates into outflows rates. Observed and simulated values of the sediment yield are shown in Figure 5.

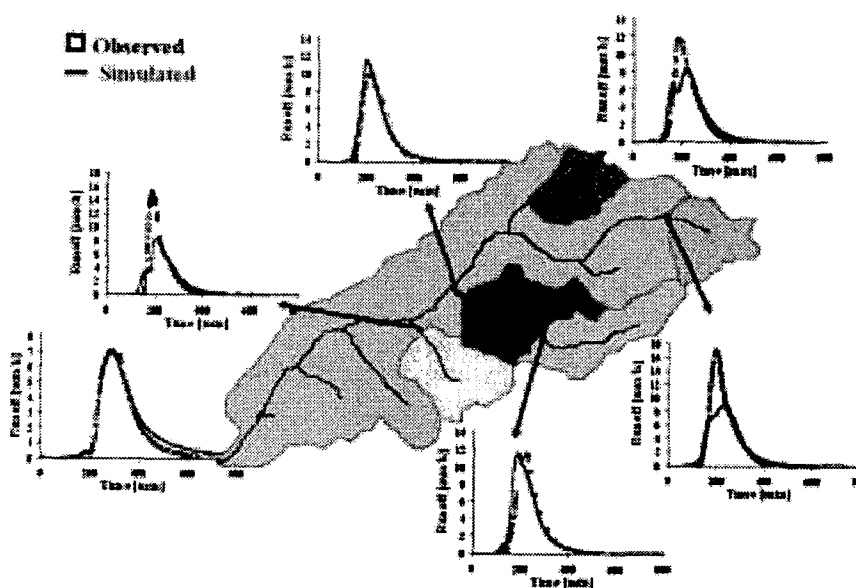


Figure 4. Observed and simulated hydrographs at the watershed outlet and at internal locations.

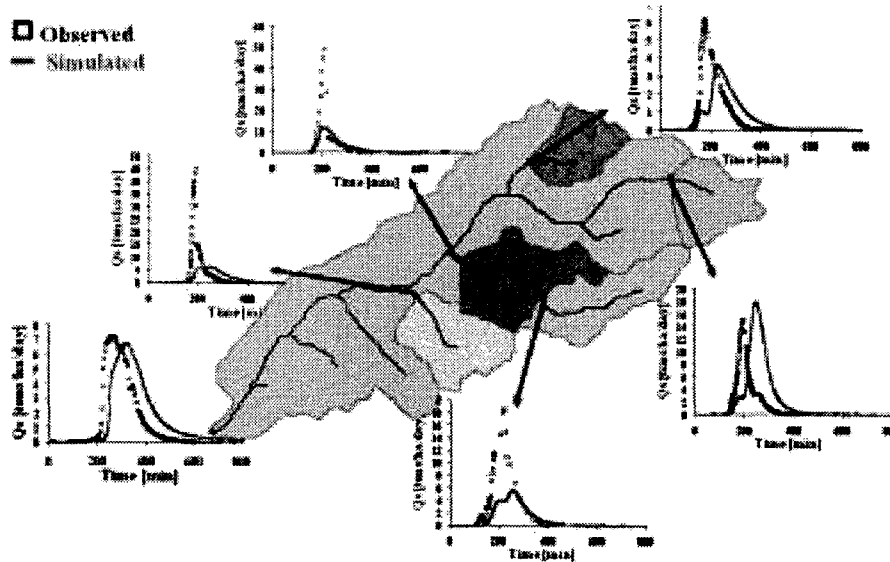


Figure 5. Observed and simulated sediment graphs at the watershed outlet and at internal locations.

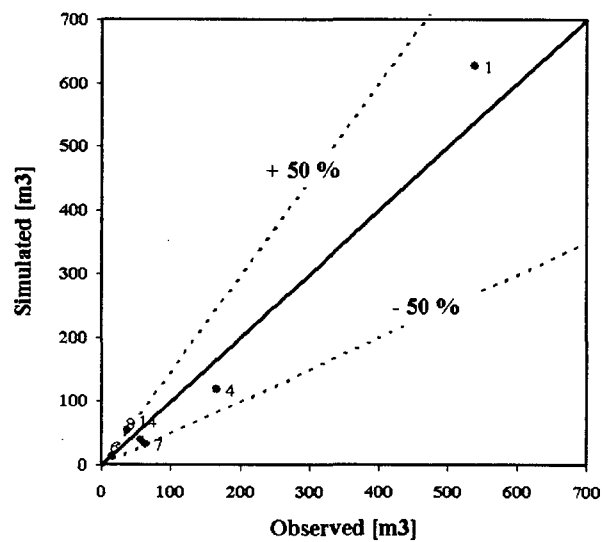


Figure 6. Observed and simulated sediment yield at the outlet (1) and other internal locations (6,7,8, and 14).

Although rising and recession limbs of the sediment graphs follow the shape of those observed, sediment outflows are locally under-predicted at internal locations. This is the subject of on-going research.

Spatially, there is practically no suspended sediment remaining at the end of the simulation but for a small amount of clay remaining in water sinks. For about half of the total eroded sediment deposits in the overland and less than 10% deposits in channels. The percentages of the total sand, silt and clay depositing on the overland are 65, 55 and 31% respectively. This is due to the differences in the settling velocities of each of the size fractions. There is no deposition of clay in channels while 25% of the eroded sand and 4% of the eroded silt deposit in the channels. The effect of both settling rates and transport capacity for each size fraction result in about 10, 40 and 70% of the total eroded sand, silt and clay respectively, to leave the watershed at the outlet. This result is comparable to observations, yet it is subject to further research.

In agreement with field observations by Johnson (1997), there are simulated zones of erosion in the pastureland along the watershed boundary, in the lower portion of the basin, and along the main stem and tributary channels. Observed areas with very little erosion within sub-basin 8 and areas of deposition between stations 14 and 2 are also in agreement to simulated values (see Figure 7). Generally, zones of high erosion are coupled with zones of deposition conditions of low slope values.

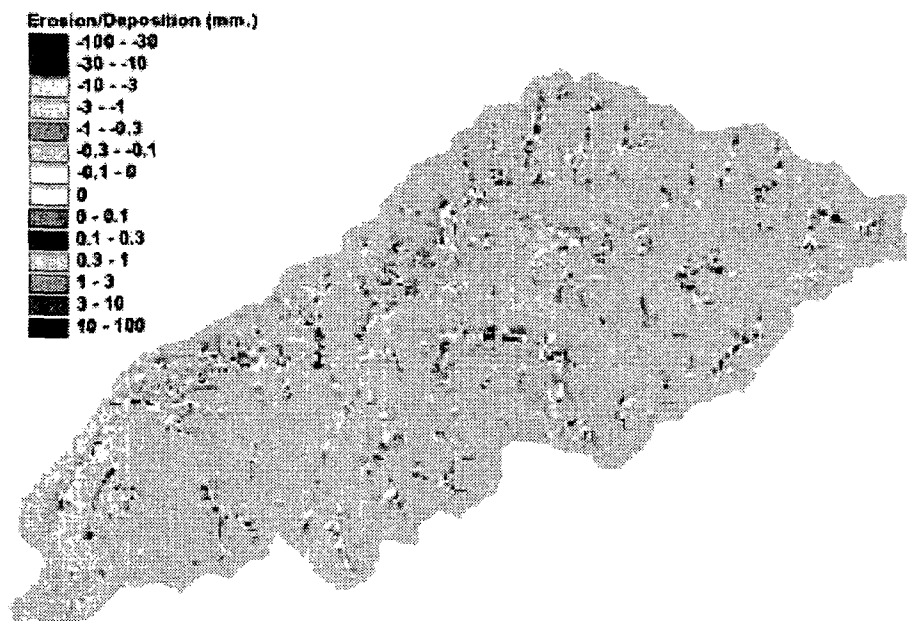


Figure 7. Net erosion volumes. Warm colors represent erosion and cold colors represent deposition.

6. Conclusions

The model CASC2D-SED was calibrated and validated on Goodwin Creek, Mississippi, using rainfall data from 16 meteorological stations and 6 stream and sediment gaging stations. Sediment erosion and deposition rates by size fraction were predicted both spatially and at internal locations. GIS was used to display dynamically the output time series grids generated by the CASC2D-SED model as an MPEG video. The following conclusions can be drawn from this study:

- CASC2D-SED is able to simulate the hydrological response of a watershed subject to a spatially and temporally variable rainfall field.
- CASC2D-SED predicts erosion and deposition zones in a watershed. The on-going research shows that these predictions qualitatively agree with the observations.
- Coupling CASC2D-SED with GIS improves the visual display of erosion and sedimentation rates and help in model verification.

Acknowledgements. Financial support was granted through the Center for Geosciences DAAL01-98-2-0078. The USDA-ARS-National Sedimentation Laboratory at Oxford (MS) provided data. Collaboration with B. Johnson, J. Jorgeson and W. Martin at ERDC-WES, Vicksburg, MS is gratefully acknowledged.

References

- Acevedo, W. and P. Masuoka, (1997), "Time-series animation techniques for visualizing urban growth," *Computers & Geosciences*, 23 (4), 423-435.
- Alonso, C. V., (1996), "Hydrologic Research on the USDA Goodwin Creek Experimental Watershed, Northern Mississippi," In Morel-Seytoux, H. J. (Ed.), *Proceedings of the 16th AGU Hydrology Days*, Colorado State University, Fort Collins, Colorado State University, 25-36.
- Blackmarr, W. A., (1995), "Documentation of Hydrologic, Geomorphic, and Sediment Transport Measurements on the Goodwin Creek Experimental Watershed, Northern Mississippi, for the Period 1982-1993 - Preliminary Release. Research Report No. 3 (CD-ROM)", U.S. Dept. of Agriculture, Agric. Research Service, 212 p.
- Brooks, S. M. and R. A. McDonnell, (2000), "Research advances in geocomputation for hydrological and geomorphological modelling towards the twenty-first century", *Hydrological Processes*, 14 (11-12), 1899-1907.
- De Roo, A. P. J., (1996), "Soil Erosion Assessment Using GIS", *Geographical Information Systems in Hydrology*; Kluwer Academic Publishers, Dordrecht, Boston, 339-356.
- Dransch, D., (2000), "The use of different media in visualizing spatial data", *Computers & Geosciences*, 26, 5-9.
- Edsall, R. M., M. Harrower and J. L. Mennis, (2000), "Tools for visualizing properties of spatial and temporal periodicity in geographic data," *Computers & Geosciences*, 26 (1), 109-118.

- Engelund, F. and E. Hansen, (1967), "A Monograph on Sediment Transport in Alluvial Stream", Teknisk Forlag, 62 p.
- Green, W. H. and G. A. Ampt, (1911),"Studies on soil physics - Part I. The flow of air and water through soils", *The Journal of Agricultural Science*, 4, 1-24.
- Haan, C. T.; B. J. Barfield and J. C. Hayes, 1994: *Design Hydrology and Sedimentology for Small Catchments*. Academic Press, 588 p.
- Johnson, B.E., P.Y. Julien, D.K. Molnar and C.C. Watson, The two-dimensional upland erosion model CASC2D-SED, *Journal of the American Water Resources Association*, AWRA, 36(1), 2000,
- Julien, P. Y., 1995: *Erosion and Sedimentation*. Cambridge University Press, 280 p.
- Julien, P. Y. and B. Saghafian, 1991: *CASC2D Users Manual - A Two Dimensional Watershed Rainfall-Runoff Model*. Civil Engineering Report, CER90-91PYJ-BS-12. Colorado State University, Fort Collins, 66 pp.
- Julien, P.Y., B. Saghafian and F.L. Ogden, *Raster-based hydrologic modeling of spatially-varied surface runoff*, *Water Resources Bulletin*, AWRA, 31(3), 1995, pp. 523-536.
- Kilinc, M. Y. and E. V. Richardson, 1973: *Mechanics of Soil Erosion From Overland Flow Generated by Simulated Rainfall*. Hydrology Papers No. 63. Colorado State University.
- Kuhnle, R. A. and J. C. Willis, 1998: *Statistics of Sediment Transport in Goodwin Creek*. *Journal of Hydraulic Engineering*, ASCE, 124 (11), 1109-1114.
- Lane, L. J.; E. D. Shirley and V. P. Singh, 1988: *Modelling Erosion on Hillslopes*. In M.G. Anderson (Ed.). *Modelling Geomorphological Systems*; Chapter 10; John Wiley & Sons; 287-308.
- Mitasova, H.; J. Jofierka; M. Zlocha and L. R. Iverson, 1996: *Modelling topographic potential for erosion and deposition using GIS*. *Int. J. Geographical Information Systems*, 10 (5), 629-641.
- Mitchell, J. K.; B. A. Engel; R. Srinivasan and S. S. Y. Wang, 1993: *Validation of AGNPS for small watersheds using an integrated AGNPS/GIS system*. *Geographic Information Systems and Water Resources*, 89-100.
- Molnar, D.K., and P.Y. Julien, 1998: *Estimation of Upland Erosion using GIS*, *Journal of Computers and Geosciences*, 24(2), 183-192.
- Molnar, D.K., and P.Y. Julien, 2000: *Grid size effects on surface runoff modeling*, *Journal of Hydrologic Modeling*, ASCE, 5(1), 8-16.
- Rawls, W. J.; D. L. Brakensiek and N. Miller, 1983: *Green-Ampt infiltration parameters from soils data*. *Journal of Hydraulic Engineering*, ASCE, 109 (1), 62-69.
- USDA, 1975: *Soil Taxonomy*. Agriculture Handbook 436, 752 p.
- Wischmeier, W. H. and D. D. Smith, 1978: *Predicting Rainfall Erosion Losses -- A Guide to Conservation Planning*. USDA Handbook No. 537.
- Woolhiser, D. A., 1975: *Simulation of Unsteady Overland Flow*. In Mahmood, K; Yevjevich, V (Eds.). *Unsteady Flow in Open Channels*; Vol. II; Water Resources Publications: Fort Collins (CO) ; p. 502.